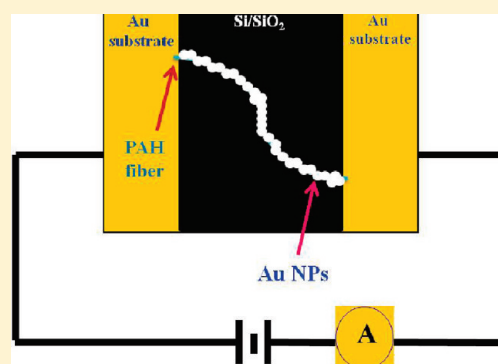


Electrospinning of PAH Nanofiber and Deposition of Au NPs for Nanodevice Fabrication

Subrata Kundu,^{†,*} Rajinder S. Gill,[‡] and Ravi F. Saraf^{*}

Department of Chemical and Biomolecular Engineering, University of Nebraska-Lincoln, NE-68588-0643, USA

ABSTRACT: A new route for the formation of electrically conductive Au-PAH composite nanofibers using electrospinning and UV-irradiation techniques is being reported. Initially, we fabricated nonwoven PAH nanofibers (diameter ~ 100 – 150 nm) using electrospinning technique. The Au nanoparticles (NPs) were synthesized and deposited in situ onto the PAH fiber in the presence of 2 h of UV photoirradiation. The diameter of these fibers and deposition of Au NPs can be tuned just by controlling the physical parameters, concentration of polymeric solution during electrospinning, the concentration of HAuCl_4 solution, and UV photoirradiation exposure time. The Au-PAH composite-based nanoelectronic device resulted in an Ohmic behavior with low resistance, confirming a continuous metallic structure. The proposed method is efficient, straightforward, reproducible, and robust. These conductive Au-PAH nanofibers can be applied for making building blocks in nanodevices and as a sensor in sensor technology.



1. INTRODUCTION

With the continuous development of nanotechnology, the study of 1D nanostructured materials like nanorods,¹ nanowires,² nanofibers,³ and nanotubes⁴ has shown great interest due to their intriguing chemical and physical properties. Among the above 1D materials, nanofibers are found more interesting due to their broad applications in nanodevice fabrication,⁵ nanoelectronics,⁶ and in sensing⁷ technology. Among the various fabrication techniques to make fibers in the submicrometer range, electrospinning is the simplest and easiest method to fabricate nanofibers. The first report on electrospinning was published by Formhals in 1934.⁸ During the electrospinning process, a strong electrostatic force is applied to the capillary containing the polymer solution. When the field strength surpasses the surface tension of the solution, the polymer solution is ejected from the tip. During the time-of-flight, the solvent is evaporated and the polymer is deposited as a nonwoven fibrous mat on a metal collector, which served as the ground for the electric charges. The fibers are collected on a ground collector and the process is very effective for the fabrication of different types of polymer, polyelectrolytes, ceramics, and biopolymers, resulting in fibers with diameters from the micrometer-to-nanometer scale range. The intrinsic properties of electrospun fibers depend on concentration, surface tension of the solvent, distance between the tip of capillary tube with the ground collector, applied voltage, humidity, and feed flow rate.

The properties of these nanofibers can be modified in a number of different ways to increase their application diversity. Incorporation of metal nanoparticles (NPs) into nanofibers generated composite nanofibers having important optical, electrical, and catalytic properties, where these composites find

applications as electronic components, optical detectors, chemical and biochemical sensors, and devices.^{3,5–10} Different types of metal NPs such as Au NPs,¹¹ Ag NPs,¹² Pd NPs,¹³ and semiconductor NPs¹⁴ were incorporated into the polymer matrix for the generation of conducting nanofibers. Among these, Au NPs have attracted increased interest by various researchers due to their well-defined optical, magnetic, and electronic properties. Kim et al. incorporated Au NPs into poly(ethylene oxide) (PEO) nanofibers by the electrospinning method.¹⁵ Han et al. assembled conductive gold films on flexibly electrospun PMMA ultrafine fibrous mat substrate containing Au NPs.¹⁶ Li et al. deposited Au NPs on the titania nanofibers by photocatalytic reduction of Au salts.¹⁷ Recently, Jian-shi et al. prepared poly(*N*-vinylpyrrolidone) (PVP) nanofibers containing Au NPs using the electrospinning method.¹⁸ Polyacrylonitrile (PAN) fibers containing Ag NPs were prepared by Wang et al.¹² Recently, the same group studied the incorporation of Au NPs in PVP nanofibers.¹⁹ Wang et al. fabricated recently a composite of Au/PVP nanofiber using electrospinning techniques.²⁰ A few other research groups were also engaged in synthesizing nanofibers containing either Au or Ag NPs.^{21–25} The incorporation of these NPs was achieved either by reducing metal salts into metal NPs in polymer solution prior to electrospinning,²¹ or by post treatment using UV radiation, heat, or chemical reduction of the electrospun polymer/metal salt composite fibers.^{22–24} It was reported that metal NPs can be synthesized on the surface of PVP fibers by taking advantage of the binding capability of pyridyl groups to metal

Received: April 26, 2011

Revised: June 26, 2011

Published: June 30, 2011

ions and NPs.²⁵ Recently, Lee et al. studied the assembly of Au nanorods on polymeric nanofibers and proposed their application as surface enhanced Raman scattering (SERS) studies.²⁶ Jacobs et al. reported that the useful applications of electrospun nanofibers requires a thorough understanding of the electrospinning parameters because the material properties at the atomic scale can be improved and modified by controlling their structural morphologies.²⁷ Han et al. synthesized uniform poly(2-aminothiophenol) nanofibers embedded with highly dispersed Au NPs using a facile templateless one-step method.²⁸

In this proposed study, we report for the first time the synthesis of electrically conductive poly(allylamine hydrochloride) and gold, (Au-PAH) composite nanofibers by exploiting the techniques of electrospinning and UV photoirradiation. Initially, we fabricated PAH nanofibers having the average diameter in 100–150 nm size range. Then, the Au NPs were synthesized using two different approaches: First being the direct synthesis in PAH solution; and, second, in situ deposition from H₂AuCl₄ solution onto the PAH fiber in the presence of UV photoirradiation for 2 h exposure. The diameter of these fibers can be tuned by controlling the physical parameters and the concentration of polymer solution to be fabricated during the electrospinning. Similarly, the deposition of Au NPs can also be controlled by altering the concentration of H₂AuCl₄ solution and the UV photoirradiation exposure time. The current process is simple, reproducible, and cost-effective. The conductive Au-PAH nanofibers might be useful for the application of making building blocks in nanoelectronics and as a sensor in sensor technology.

2. EXPERIMENTAL SECTION

2.1. Reagents. Polyallylamine hydrochloride (PAH), dodecyl trimethylammonium bromide (DTAB-99%) and hydrogen chloroauric acid (H₂AuCl₄·3H₂O) were purchased from Aldrich-Sigma and used as received. Deionized (DI) water was used for any type of wet chemistry and processing.

2.2. Instruments. A custom-built electrospinning setup was used for the nanofabrication of PAH where the feed flow rate was precisely controlled using a syringe pump purchased from Cole-Parmer. The UV–vis absorption spectra were recorded in an ocean-optics absorbance spectrophotometer (model number USB4000) equipped with 1 cm quartz cuvette holder for liquid samples. The instrument offers a wide wavelength of 190–1100 nm range. Transmission electron microscopy (TEM) analysis was performed using a Hitachi-H-9000 NAR. The samples for TEM were prepared by placing a droplet of fresh Au NPs solution onto carbon-coated copper grid followed by slow evaporation of solvent at ambient conditions. The energy dispersive spectroscopy (EDS) analysis was performed with the same instrument having the TEM/EDS capabilities. The field emission scanning electron microscope (FESEM) analysis was performed using a Hitachi S-4700. FESEM studies were performed on Si-chip coated with Au lines with a protective oxide layer on the Si surface. The chip was cleaned thoroughly with ethanol and piranha (30% H₂O₂ and 70% H₂SO₄) followed by final cleaning with ethanol and acetone. The chip was dried and placed in Au NPs solution for 30 min to deposit Au NPs. The XRD analysis was conducted at a scanning rate 0.020 S-1 in the 2θ range 30–85° using a Rigaku D_{max} γ_A X-ray diffractometer with Cu–Kα radiation (λ = 0.154178 nm). A xenon lamp source (Newport Corp.) was used to generate UV-photoirradiations with 260–270 nm wavelength range and were aimed at the

sample. The approximate intensity of the irradiation was 2 μW and the distance of the sample from the light source was 12 cm. The sample was placed over a small wooden box with a stand to focus the light directly onto the sample.

2.3. Solution Phase Synthesis of PAH-Au NPs Using UV Photoirradiation. An aqueous solution of PAH solution (0.1% by weight) was prepared by dissolving in DI water and stirring for about 10 h. A stock solution of 10⁻² M chloroauric acid (H₂AuCl₄·3H₂O) was prepared, diluted to a concentration of 1.23 × 10⁻⁴ M, and kept under dark for protection against light. In a typical synthesis, 4 mL of PAH (0.1%) solution were mixed with 2 mL of (1.23 × 10⁻⁴ M) chloroauric acid solution and the mixture was stirred for 2–3 min using magnetic stirrer and allowed it to equilibrate for ~2 min. The resulting solution was UV-irradiated continuously for 2 h. The formation of Au particles started after 30 min of UV irradiation and the synthesis was completed after 2 h. This was confirmed based on the visual observation of color change, as well as UV–vis spectrum. The color of the final Au NPs solution was reddish pink, which remained stable for more than six months in ambient environment without a change in optical properties. The Au NPs solution was characterized using UV–vis, TEM, EDS, and XRD analysis.

2.4. Fabrication of PAH Nanofiber by Electrospinning Method. An aqueous solution of poly(allylamine) hydrochloride (PAH) (25 wt %) was prepared using DI water. Approximately 5–9 wt % of cationic surfactants, dodecyltrimethylammonium bromide (DTAB) was added to the PAH solution. It was reported in previous studies that surfactants (nonionic, anionic, or cationic) have been used extensively to lower the surface tension of aqueous solutions.^{29–31} The main use of DTAB in our formulation was to lower the surface tension of PAH aqueous solution, which was required for the fabrication of PAH fibers and also helped to attain stable Taylor cone during electrospinning. The stability of Taylor cone is important for obtaining uniform fibrous material within controlled diameter and narrow size range. The PAH solution was fed through a syringe at a volumetric flow rate of 0.3 mL/h. The chip was mounted on the collector which was placed at approximately 28 cm from the tip of the capillary needle and the voltage in the range of 20–22 kV was applied across the needle and collector. The fibers so produced were collected on the chip, which was mounted on the collector. In some cases, the alignment of the fibers was controlled using the rotating drum and is used as the collector. PAH has been fabricated as thin layers leading to multilayer devices for sensing applications. PVP/Au nanofibers were fabricated by Wang et al.²⁰ in a similar way. Recently, few other groups fabricated polymer nanofibers using the techniques of layer-by-layer electrostatic self-assembly of oppositely charged polymers.^{32,33} The chemical nature of polymers and its reducing capability has been exploited for the fabrication of nanocomposites using electrospinning technique. For conductivity study, PAH fibers were collected on a specially designed Si/SiO₂ chip, containing multiple gold pads, which were separated from each other with varying gaps ranging from 5 to 50 μm. The fibers collected on the chip were baked in an oven at 130 °C for an hour under vacuum. It is important to note that there was no significant change in fiber morphology after baking at 130 °C. The main reason for baking PAH nanofibers was to evaporate solvent and increase adhesion onto the substrate. It has been reported by Kameoka et al.,³⁴ Samuel et al.,³⁵ and Zhao et al.³⁶ that fibrous or layered structures of polymers and polyelectrolytes retain their morphologies and

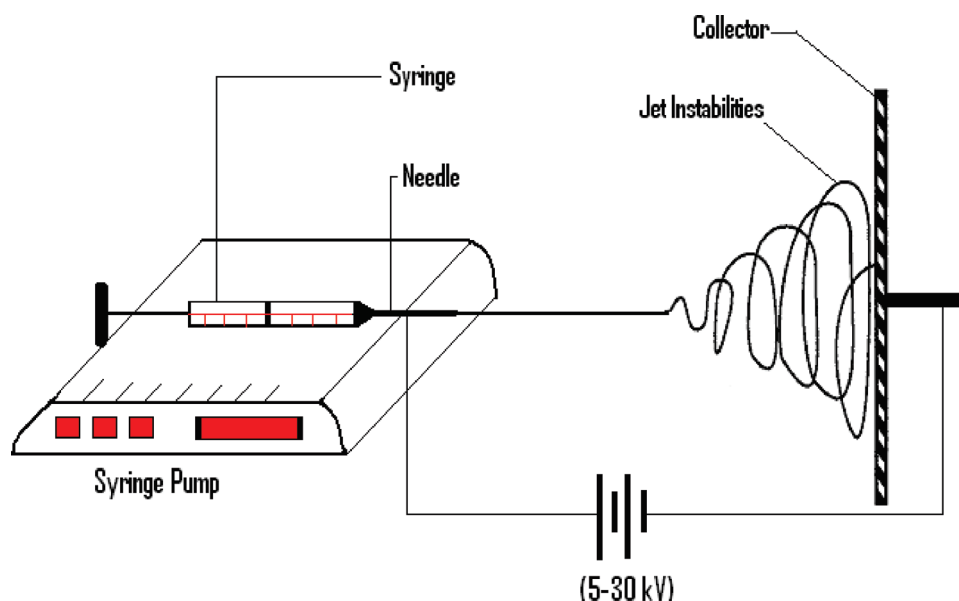


Figure 1. Schematic presentation for the electrospinning set up process.

electronic structure when exposed to temperatures below 140 °C during solvent evaporation. The dried sample was then rinsed with water and used for Au NPs deposition. Finally, the samples were characterized using FE-SEM. The interactive drawing for the electrospinning set up is shown in Figure 1.

2.5. In-Situ Synthesis and Deposition of Au NPs on PAH Fiber by UV-Photoirradiation. The PAH nanofibers were collected on a designed Si-chip containing Au lines/pads separated by a specified gap. The gap between the two gold pads varied from 5 to 50 μm . The chip containing the PAH nanofibers was immersed in a solution containing 2 mL of 1.23×10^{-4} M HAuCl_4 solution and 2 mL of DI water. Then the solution containing the chip and HAuCl_4 solution were exposed directly to the UV-photoirradiation source for 2 h continuously. After 2 h of UV exposure, the chip was removed from the solution and rinsed with DI water very gently and then dried. The dried chip containing the fiber and Au NPs was characterized and tested using FESEM and current–voltage (I–V) measurements.

2.6. Preparation of Samples for TEM, EDS, XRD, FE-SEM, and I–V Studies. The samples for TEM and EDS analysis were prepared by placing a drop of corresponding PAH-Au NPs solution onto a carbon-coated Cu grid, followed by slow evaporation of solvent at ambient conditions. For XRD analysis, silicon (Si) wafers were used as the substrate for thin film preparation. The wafers were cleaned thoroughly in acetone and sonicated for about 20 min. The cleaned substrates were covered with PAH-Au NPs solution and dried in a vacuum chamber. After the first layer was deposited, subsequent layers were deposited repeatedly by adding more Au NP solution and then the samples were dried. Final samples were obtained after 8 iterations of these depositions, and then analyzed using XRD techniques. For FE-SEM and I–V studies, the Au NPs were directly deposited on solid substrate containing the PAH nanofibers using UV photoirradiation for 2 h continuously.

3. RESULTS AND DISCUSSION

3.1. UV–Vis Spectroscopic Study and Transmission Electron Microscopy (TEM) Analysis. A mixture of an aqueous

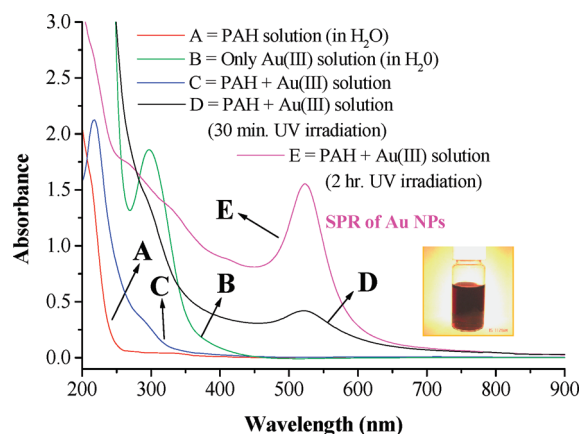


Figure 2. UV–vis spectrum for the formation of PAH-Au NPs. (A) is the absorption spectrum for aqueous PAH solution. (B) is the absorption spectra of aqueous HAuCl_4 solution which shows an absorption band at ~ 297 nm. (C) is the absorption spectrum of a mixture of PAH and HAuCl_4 . (D) is the surface Plasmon resonance (SPR) band of Au NPs solution after 30 min of UV-irradiation. (E) is the SPR band of Au NPs solution after 2 h of UV-irradiation, shows a peak at 522 nm. Inset shows the pink color PAH-Au NPs solution.

solution of PAH (0.1%) and an aqueous solution of HAuCl_4 resulted in pink color Au NPs solution when irradiated with UV light for 2 h continuously. During the synthesis of these Au NPs, PAH plays a dual role. It serves not only as a reducing agent during the synthesis process but also acts as a stabilizing agent after the formation of Au particles. The detailed mechanism of the particles formation is discussed later. Figure 2 shows the UV–vis spectrum for the formation of PAH-Au NPs. Part A of Figure 2 is the absorption spectrum for aqueous PAH solution only. Part B of Figure 2 is the absorption spectra of aqueous HAuCl_4 solution, which shows an absorption band at ~ 297 nm due to metal-to-ligand charge transfer (MLCT) spectra.³⁷ Part C of Figure 2 represents the absorption spectrum of a mixture of PAH and HAuCl_4 . It was observed that there is a shift and change

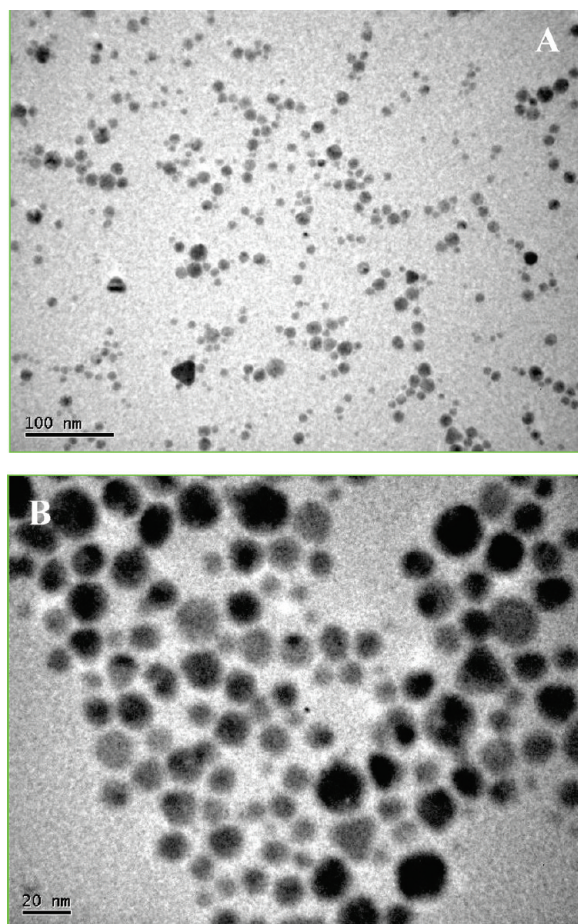


Figure 3. The transmission electron microscopy (TEM) images of the PAH-Au NPs. (A) is the low magnified image and (B) is the high magnified image. The average diameter of the particles are $\sim 10\text{--}15$ nm.

in absorption value, which confirmed instantaneous formation of PAH-Au (III) complex. The Au NPs formation started after 30 min of UV-irradiation as shown by a small surface Plasmon resonance (SPR) peak appeared at 522 nm (spectrum D, Figure 2). The color of the resulting solution became light pink. Now after 2 h of UV-irradiation, the mixture resulted into deep-pink color Au NPs solution as shown by a high intense SPR band in spectrum E, Figure 2. This spectrum shows an absorption maximum at 522 nm due to SPR of spherical Au NPs solution.^{38–40} An inset of Figure 2 shows the pink-colored spherical PAH-Au NPs solution. The TEM images of the PAH-Au NPs are shown in Figure 3. Part A of Figure 3 shows the low magnified image, whereas part B shows the high magnified image. From the image, it is evident that the average diameters of these Au NPs are approximately 10–15 nm. The particles were monodispersed, well separated from each other, and did not undergo any agglomeration during synthesis.

3.2. Scanning Electron Microscopy (SEM) Analysis. We have demonstrated that the reaction of PAH with HAuCl_4 in the presence of UV light produced Au NPs in solution within the narrow size range. Using an alternate approach, we tried in situ deposition of Au NPs directly onto PAH nanofibers. We fabricated PAH nanofibers by electrospinning method, which is discussed in detail in the Experimental section. PAH fibers were

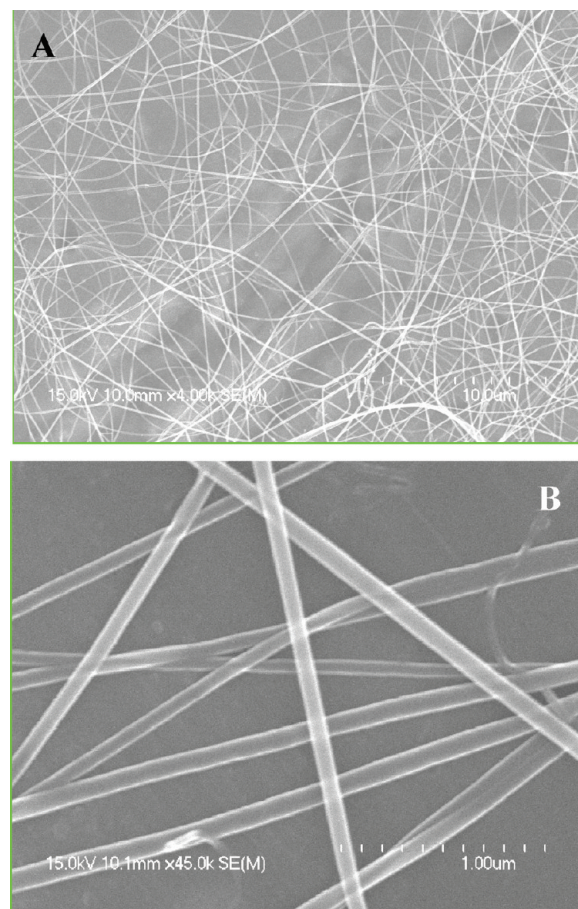


Figure 4. Scanning electron microscopy (SEM) images of the PAH nanofibers at different magnification. (A) is the low magnified SEM image and (B) is the high magnified image of PAH nanofiber.

collected and deposited on a specially designed Si/SiO₂ chip coated with conducting Au lines, which were separated from each other with a specific and precise gap. The gap between two conducting lines varied from 5 to 50 μm . The chip containing PAH fibers was immersed in a small quartz cuvette containing the Au (III) solution. The sample was exposed to UV-irradiation for 2 h continuously, and then the chip was removed from the Au (III) solution, followed by rinsing with water and then dried. This dried sample was analyzed using various characterization techniques. Figure 4 shows the scanning electron microscopy (SEM) images of the PAH nanofibers at different magnification. Part A of Figure 4 shows the low magnified SEM image, whereas part B of Figure 4 shows the high magnified SEM image. From these images, it can be interpreted that majority of the fibers were in the narrow size range of 100–150 nm. Figure 5 shows the SEM images of the PAH fibers at different stages of Au NPs deposition. Part A of Figure 5 is the SEM image when Au NPs were deposited for 1 h UV-irradiation. From these images, it can be interpreted that Au NPs were formed in the solution and were deposited selectively onto the PAH nanofibers. Part B of Figure 5 represents the SEM image after 2 h of UV irradiation exposure. It can be clearly observed from these images that Au NPs that were formed due to UV-irradiation of the solution containing PAH fiber and HAuCl_4 solution were selectively deposited onto the PAH fiber. It was evident that the deposition of Au NPs was selective and deposited only on PAH fibers. This is mainly due to

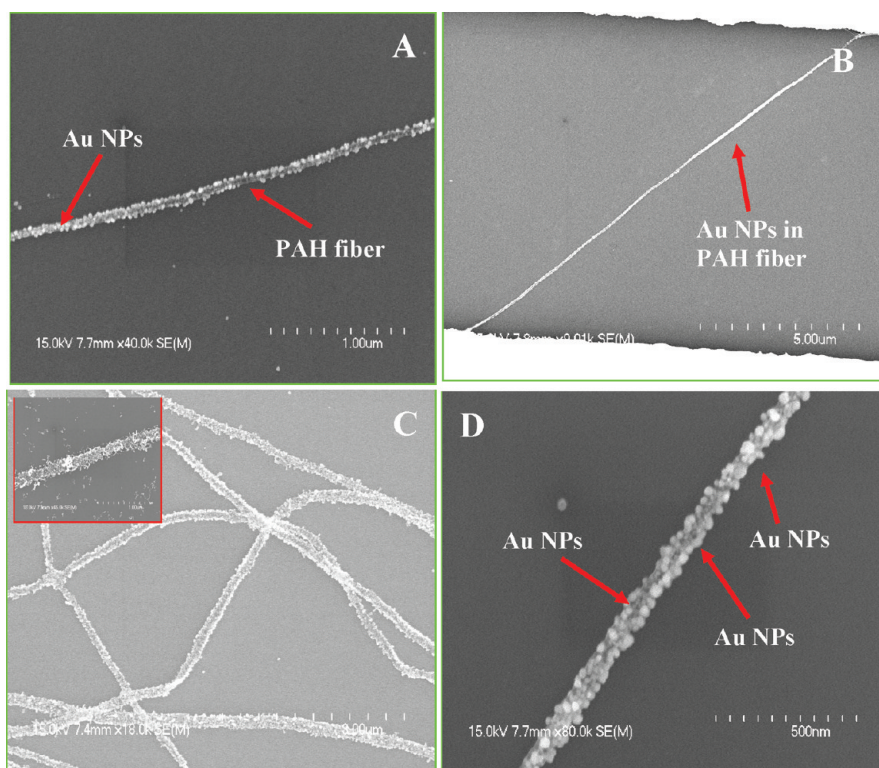


Figure 5. SEM images of the PAH fibers at different stages of Au NPs deposition. (A), (B), and (C) are the SEM image of the PAH fiber when Au NPs are deposited for 1 h, 2 h, and 4 h UV-irradiation respectively. Inset of (C) shows the corresponding high magnified image. (D) show the high magnified image of the PAH fiber when Au NPs are deposited for 2 h of UV-irradiation.

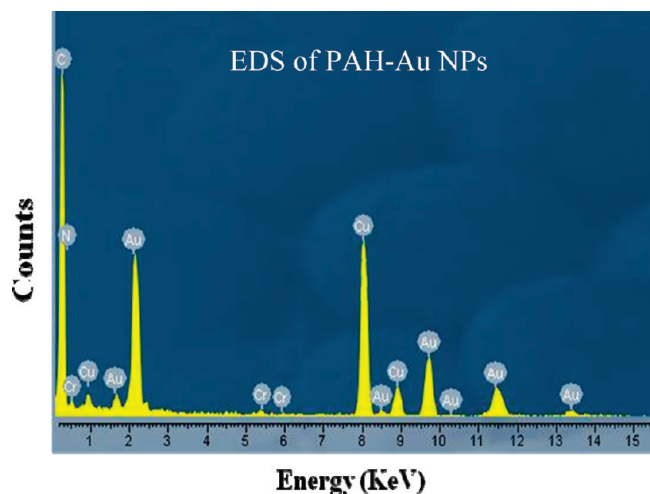


Figure 6. Energy dispersive X-ray spectroscopic (EDS) analysis of the PAH-Au nanofibers. The spectrum shows the expected peaks for Au, Cu, C, and N.

the electrostatic interaction between the positively charged polymers and negatively charged gold ions. Part C of Figure 5 represents the SEM image where Au NPs were synthesized on PAH fibers using 4 h of UV-irradiation exposure time. It can be observed that 4 h of UV exposure resulted in an excess deposition of Au particles onto the PAH fiber. Some of the Au NPs resulted in branchlike morphologies that can be observed at higher magnification in an inset of part C of Figure 5. Part D of Figure 5 represents the higher magnification image of the same sample which was exposed to 2 h of UV-irradiation (part B of Figure 5).

It was observed that the Au NPs were formed in solution and deposited uniformly after 2 h of continuous UV-irradiation. On the basis of this analysis, UV-irradiation exposure time was optimized for 2 h to obtain uniform deposition of Au NPs onto the PAH fiber. It can be interpreted from part D of Figure 5 that the Au NPs were synthesized, deposited uniformly and selectively onto PAH fibers.

3.3. Energy Dispersive X-ray Spectroscopy (EDS) Analysis.

Au-PAH composite was analyzed for its elemental composition using Energy Dispersive X-ray Spectroscopic (EDS) and the scan is shown in Figure 6. The spectrum shows the presence of Au, Cu, C, and N. The Au peak come from the Au NPs, whereas the N peak appeared due to presence of amino group in the PAH fibers. The C and Cu peak is due to the carbon coating of Cu TEM grid, which was used for sample preparation.

3.4. X-ray Diffraction (XRD) Analysis. The X-ray diffraction (XRD) pattern of the PAH-Au nanofiber is shown in Figure 7. The diffraction pattern consisted of diffraction from (111), (200), (220), (311), and (222) planes, which can be attributed to the fcc structure of Au NPs. The calculated lattice constant for the Au NPs was 0.406 nm, which is consistent and in agreement to the numbers reported in literature ($a = 0.4077$ nm, as reported by JCPDS file number 4-0784).⁴¹ From these analyses, it was confirmed that the Au NPs were formed in the solution and deposited selectively on the PAH fiber. The resulting device was found out to be stable and robust. The detailed mechanism of their formation is discussed in section 3.5.

3.5. Mechanism of the Au NPs Formation and Their Deposition on Fiber. Using 2 h of UV-irradiation exposure time, Au NPs were synthesized not only in an aqueous PAH solution but also directly onto the PAH fibers which were

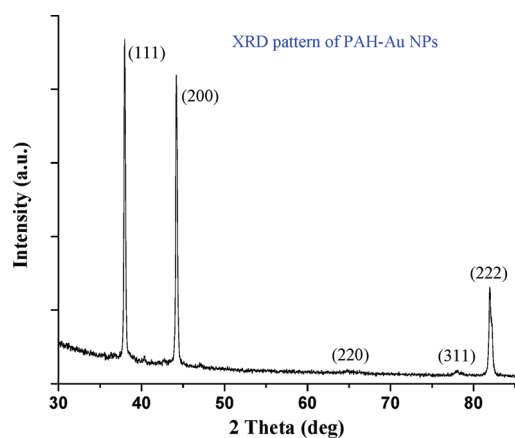


Figure 7. X-ray diffraction (XRD) pattern of the PAH-Au nanofiber shows the diffraction from the (111), (200), (220), (311), and (222) planes of fcc Au NPs.

deposited across Au pads on a Si-chip. During the synthesis process, the presence of both PAH and UV-photoirradiation is important. PAH contributes to the formation of small monodisperse nanoparticles. In the absence of PAH, keeping all other parameters the same, solution resulted in micrometer size particles that agglomerate immediately after their formation. In the absence of UV photoirradiation, Au NPs were not formed. During this synthesis, PAH acts as a reducing agent for the reduction of AuCl_4^- to $\text{Au}(0)$. The amino ($-\text{NH}_2$) group in the PAH acts as a reducing agent for this reduction. It was reported previously that the amine group can reduce the metal ions and oxidize itself to imine.⁴² During the formation of Au NPs in solution, the positively charged polymer first formed a complex with AuCl_4^- that can be proved from the UV-vis spectrum (part C of Figure 2). Then, in the presence of UV-irradiation, electron transfer process is initiated from the polymer to the Au^{3+} and then, Au^{3+} was reduced to $\text{Au}(0)$.⁴³ Initially, Au nuclei were formed during the reduction process. These Au nuclei subsequently contribute to the formation of Au atoms and then aggregate together to form crystalline particles. In our present case, at a particular concentration of PAH, the growth takes place in all possible directions and generates spherical Au NPs. Although, from the high magnified SEM images, a few chainlike morphologies at a few spots in the sample were also observed. The polymer adsorbs onto the surface of the crystalline particles, control their growth, and inhibit the agglomeration of the fully grown particles. The amino group ($-\text{NH}_2$) of PAH coordinated via the nitrogen atom to the formed Au NPs and stabilized them in the solution. The allyl amine chain becomes confined in the outer shell of the polymer micelles and generates a hydrophobic environment for the NPs. Minko et al.⁴⁴ and Kuo et al.⁴³ also observed similar types of electron transfer reaction from the polymer to the metal ions during the synthesis of NPs. During the formation of Au NPs on PAH fiber, the formation mechanism is also similar to that of the solution cast method. Dong et al. studied the assembly of Ag, Au, and Pt NPs over electrospun nylon 6 nanofibers by controlling their interfacial hydrogen bonding interaction.⁴⁵ They observed that a large number of NPs assemble on fiber when pH of the solution was kept between 3 and 6. In other cases, limited surface coverage was noticed. But in our study we observed from the SEM images in part B of Figure 5 that the NPs were synthesized selectively only onto the

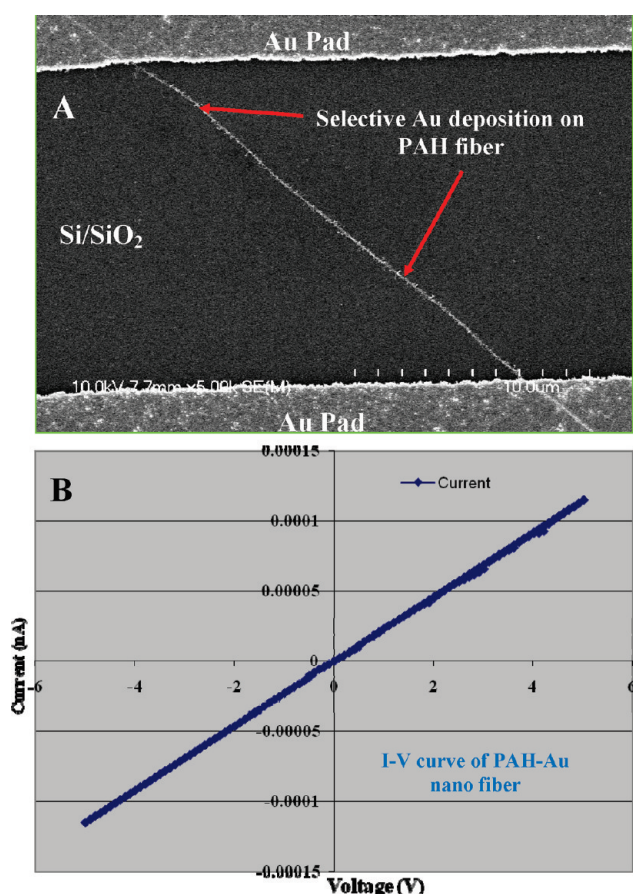
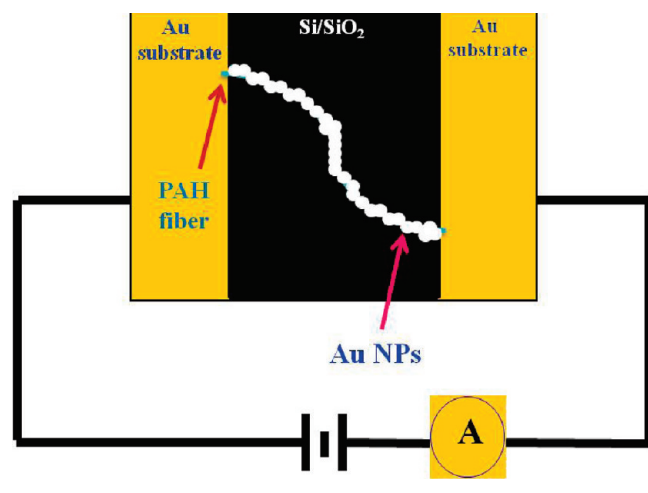


Figure 8. (A) Shows the SEM image of the PAH-Au nanofiber deposited on the substrate for the conductivity measurement. (B) Shows the I-V curve of the PAH-Au nanofiber. From the linear fit I-V curve, the resistance of the nanofiber is $447.6 \times 10^{11} \Omega$.

fiber not other part of the samples. This is due to the presence of PAH, which acts not only as a reducing agent but also as stabilizing agents after the formation of smaller Au NPs. The smaller Au NPs were formed, where they aggregate and grow on the PAH fiber to produce Au NPs deposited onto PAH nanofiber. This in situ process for the synthesis of Au NPs selectively on PAH fiber is the first example for the development of Au-PAH nanoelectronic device. This study concludes that Au NPs can be synthesized either in the solution or on the solid substrate in presence of PAH. The formation of Au NPs by the reduction of HAuCl_4 with NaBH_4 or with different amine compounds has been reported.^{42,46-48} The appearance of stretching vibration absorption of C-N double bond ($-\text{N}=\text{C}-$) peak around 1615 cm^{-1} in FTIR analysis indicated that the oxidation of amines to imines. In this article, our focus was to fabricate polyelectrolyte (PAH) and then in situ synthesis and deposition of Au NPs to develop a conducting nanodevice and test for its optoelectronic properties. After the complete coverage of the fiber by the NPs, the electrical conductivity measurements were performed to validate the system for device application.

3.6. Conductivity (I-V) Study. We measured the conductivity of the resulting nanoelectronic device where Au-coated PAH nanofiber was used to bridge Au pads spaced $20 \mu\text{m}$ apart on a Si chip. After the synthesis, the chip was dried in vacuum and I-V measurement was conducted with a pair of Au electrode on a custom-built system. The gap between two Au bridges can be

Scheme 1. Schematic Drawing for the I–V Measurement on PAH-Au Nanofiber



varied from 5 to 50 μm , which can be designed during manufacture of the chips. Here, we studied the conductivity keeping 20 μm gap between the two gold pads. Part A of Figure 8 shows the SEM image of the Au-PAH nanofiber deposited on the substrate for the conductivity measurement. Scheme 1 shows the schematic of the I–V measurement on Au-PAH nanofiber. The results of the current–voltage (I–V) measurements across the PAH-Au nanofiber are shown in part B of Figure 8. From the I–V curve, it can be concluded that the nanofiber exhibit Ohmic behavior and the absence of hysteresis confirmed a continuous metallic structure. Guo et al.⁴⁹ reported the resistance of ZnO nanofiber to be around $3.5 \times 10^7 \Omega$. In our study, from the linear fit of I–V curve, it was found that the resistance of the nanofiber is $447.6 \times 10^{11} \Omega$, which is more than reported by Guo et al. During I–V testing, it was found that Au pads when bridged with uncoated PAH fibers were nonconductive. Moreover, when our system was bridged with low density uncoated PAH fibers were also nonconductive even at high voltages (~ 30 – 40 V) during I–V testing, whereas the conductance of PAH/Au nanocomposites is shown in part B of Figure 8. It was found that, for any Au pad to be conductive, it requires a uniform and highly dense NPs deposition. The present process summarizes the synthesis of PAH fiber by electrospinning method and in situ deposition of Au NPs selectively in the fiber using UV-irradiation techniques. This process provided a new route for the fabrication of other polymers and their conjugation with other metal NPs for future applications as nanoelectronic devices and sensors.

4. CONCLUSIONS

In conclusion, we have demonstrated a new route for the formation of electrically conductive PAH-Au composite nanofiber by exploiting the techniques of electrospinning and UV photoirradiation. We fabricated the PAH nanofibers having diameter in the ~ 100 – 150 nm size range. The Au NPs are synthesized either directly in PAH solution or deposited selectively in situ onto the PAH fiber in the presence of 2 h of UV-photoirradiation. The diameter of the fiber can be tuned by controlling the physical parameters or by the concentration of polymeric solution during electrospinning. Similarly, the deposition of Au NPs can also be controlled by altering the concentration of HAuCl_4 solution and

UV photoirradiation exposure time. The Au-PAH composite-based nanodevice showed an Ohmic behavior with low resistance and the absence of hysteresis in the I–V curve confirmed a continuous metallic structure. This process is efficient, straightforward, reproducible, and robust. This process provides a new route for the development of building blocks in wire electronic nanodevices, microelectronics industry, and as a sensor in sensor technology.

AUTHOR INFORMATION

Corresponding Author

*E-mail: subrata_kundu2004@yahoo.co.in (S.K.); rsaraf@unlnotes.unl.edu, Phone: 402-472-8284, Fax: 402-472-6989 (R.F.S.).

Present Addresses

[†]Electrochemical Materials Science (ECMS) Division, Central Electrochemical Research Institute (Council of Scientific and Industrial Research), Karaikudi-630006, Tamil Nadu, India.

[‡]Alloy Surfaces Technology Center, 1515 Garnet Mine Road, Boothwyn, PA- 19060, USA.

ACKNOWLEDGMENT

Financial support from NSF (NER-0608877) is appreciated.

REFERENCES

- Jana, N. R.; Gearheart, L. A.; Murphy, C. J. *J. Phys. Chem. B* **2001**, *105*, 4065.
- Kundu, S.; Liang, H. *Langmuir* **2008**, *24*, 9668.
- Dzenis, Y. *Science* **2004**, *304*, 1917.
- Oshima, Y.; Onga, A.; Takayanagi, K. *Phys. Rev. Lett.* **2003**, *91*, 205503.
- Yang, X.; Guillorn, M. A.; Austin, D.; Melechko, A. V.; Cui, H.; Meyer, H. M., III; Merkulov, V. I.; Caughman, J. B. O.; Lowndes, D. H.; Simpson, M. L. *Nano Lett.* **2003**, *3*, 1751.
- Liu, L.; Zhao, Y.; Jia, N.; Zhou, Q.; Zhao, C.; Yan, M.; Jiang, Z. *Thin Solid Films* **2006**, *503*, 241.
- Yang, Y.; Fan, X.; Long, Y.; Su, K.; Zou, D.; Li, N.; Zhou, J.; Li, K.; Liu, F. *J. Mater. Chem.* **2009**, *19*, 7290.
- Formhals, A. U.S. Patent, 1975504, 1934.
- Islam, M. R.; Podder, J. *Cryst. Res. Technol.* **2009**, *44*, 286.
- Baker, R. T. K.; Rodriguez, N.; Mastalir, A.; Wild, U.; Schlögl, R.; Woosch, A.; Paál, Z. *J. Phys. Chem. B* **2004**, *108*, 14348.
- Tseng, R. J.; Huang, J.; Ouyang, J.; Kaner, R. B.; Yang, Y. *Nano Lett.* **2005**, *5*, 1077.
- Wang, Y.; Yang, Q.; Shan, G.; Wang, C.; Du, J.; Wang, S.; Li, Y.; Chen, X.; Jing, X.; Wei, Y. *Mater. Lett.* **2005**, *59*, 3046.
- Kim, C.; Kim, Y. A.; Kim, J. H.; Kataoka, M.; Endo, M. *Nanotechnology* **2008**, *19*, 145602.
- Dong, F.; Li, Z.; Huang, H.; Yang, F.; Zheng, W.; Wang, C. *Mater. Lett.* **2007**, *61*, 2556.
- Kim, G.; Wutzler, A.; Radosch, H.; Michler, G. H.; Simon, P.; Sperling, R. A.; Parak, W. J. *Chem. Mater.* **2005**, *17*, 4949.
- Han, G. Y.; Guo, B.; Zhang, L. W.; Yang, B. S. *Adv. Mater.* **2006**, *18*, 1709.
- Li, D.; McCann, J. T.; Gratt, M.; Xia, Y. N. *Chem. Phys. Lett.* **2004**, *394*, 387.
- Jian-shi, D.; Qian-biao, Y.; Jie, B.; Shu-gang, W.; Chao-qun, Z.; Yao-xian, L. *Chem. Res. Chinies U.* **2007**, *23*, 538.
- Wang, Y.; Li, Y.; Sun, G.; Zhang, G.; Liu, H.; Du, J.; Yang, S.; Bai, J.; Yang, Q. *J. Appl. Phys.* **2007**, *105*, 3618.
- Wang, Y.; Li, Y.; Sun, G.; Zhang, G.; Liu, H.; Du, J.; Yang, S.; Bai, J.; Yang, Q. *J. Appl. Polym. Sci.* **2007**, *105*, 3618.

- (21) Yang, Q. B.; Li, D. M.; Hong, Y. L.; Li, Z. Y.; Wang, C.; Qiu, S. L.; Wei, Y. *Synth. Met.* **2003**, *137*, 973.
- (22) Son, W. K.; Youk, J. H.; Lee, T. S.; Park, W. H. *Macromol. Rapid Commun.* **2004**, *25*, 1632.
- (23) Xu, X. Y.; Yang, Q. B.; Wang, Y. Z.; Yu, H. J.; Chen, X. S.; Jing, X. B. *Eur. Polym. J.* **2006**, *42*, 2081.
- (24) Hong, K. H.; Park, J. L.; Sul, I. H.; Youk, J. H.; Kang, T. J. *J. Polym. Sci., Part B: Polym. Phys.* **2006**, *44*, 2468.
- (25) Dong, H.; Fey, E.; Gandelman, A. *Chem. Mater.* **2006**, *18*, 2008.
- (26) Lee, C. H.; Tian, L.; Abbas, A.; Kattumenu, R.; Singamaneni, R. *Nanotechnology* **2011**, *22*, 275311.
- (27) Jacobs, V.; Anandjiwala, R. D.; Maaza, M. *J. Appl. Polym. Sci.* **2010**, *115*, 3130.
- (28) Han, J.; Dai, J.; Li, L.; Fang, P.; Guo, R. *Langmuir* **2011**, *27*, 2181.
- (29) Lin, T.; Wang, H.; Wang, H.; Wang, X. *Nanotechnology* **2004**, *15*, 1375.
- (30) Deo, P.; Deo, N.; Somasundaran, P. *Langmuir* **2007**, *23*, 5906.
- (31) Ishida, T.; Okamoto, S.; Makiyama, R.; Haruta, M. *Appl. Catal., A* **2009**, *353*, 243.
- (32) Goicoechea, J.; Zamarreño, C.; Matias, I.; Arregui, F. *Sens. Actuators, B* **2008**, *132*, 305.
- (33) Poghosian, A.; Abouzar, M. H.; Amberger, F.; Mayer, D.; Han, Y.; Ingebrandt, S.; Offenhäusser, A.; Schöning, M. J. *Biosens. Bioelectron.* **2007**, *22*, 2100.
- (34) Kameoka, J.; Verbridge, S. S.; Liu, H.; Czaplewski, D. A.; Craighead, H. G. *Nano Lett.* **2004**, *11*, 2105.
- (35) Samuel, B. A.; Haque, M. A.; Yi, B.; Rajagopalan, R.; Foley, H. C. *Nanotechnology* **2007**, *18*, 115704.
- (36) Zhao, H.; Wu, X.; Tian, W.; Ren, S. *Adv. Mater. Res.* **2010**, *150–151*, 1480.
- (37) Roy, Meson, W.; Gray, H. B. *Inorg. Chem.* **1968**, *7*, 55.
- (38) Kundu, S.; Maheshwari, V.; Saraf, R. F. *Langmuir* **2008**, *24*, 551.
- (39) Kundu, S.; Peng, L.; Liang, H. *Inorg. Chem.* **2008**, *47*, 6344.
- (40) Kundu, S.; Lau, S.; Liang, H. *J. Phys. Chem. C* **2009**, *113*, 5150.
- (41) Guinier, A. *X-Ray Diffraction*; W. H. Freeman: San Francisco, CA, 1963.
- (42) Keene, F. R. *Coord. Chem. Rev.* **1999**, *187*, 121.
- (43) Kuo, P. L.; Chen, C. C.; Jao, M. W. *J. Phys. Chem. B* **2005**, *109*, 9445.
- (44) Minko, S.; Kiriya, A.; Gorodyska, G.; Stamm, M. *J. Am. Chem. Soc.* **2002**, *124*, 10192.
- (45) Dong, H.; Wang, D.; Sun, G.; Hinestroza, J. P. *Chem. Mater.* **2008**, *20*, 6627.
- (46) Kotz, J.; Kosmella, S.; Beitz, T. *Prog. Polym. Sci.* **2001**, *26*, 1199.
- (47) Kinyanjui, J.; Hanks, J.; Hatchett, D.; Smith, A.; Josowicz, M. *J. Electrochem. Soc.* **2004**, *151*, D113.
- (48) Newman, J.; Blanchard, G. J. *Nanopart. Res.* **2007**, *9*, 861.
- (49) Guo, J.; Song, Y.; Chen, D.; Jiao, X. *J. Dispersion Sci. Technol.* **2010**, *31*, 684.